Nanoparticle-induced phenomena in polyurethanes

6

*D.K. Patel, A. Biswas, P. Maiti**
School of Material Science and Technology, Indian Institute of Technology (BHU), Varanasi, Uttar Pradesh, India
*Corresponding author: pmaiti.mst@itbhu.ac.in

6.1 Introduction

Polyurethanes (PUs), versatile polymeric materials, are used extensively in biomedical applications due to their excellent biocompatibility, processability, and exceptional mechanical flexibility [1,2]. PUs are widely used as adhesives, coatings, construction materials, synthetic leathers, flame retardants, and wound dressings. PUs can be tailored in terms of their mechanical properties, oxygen permeability, barrier properties, and drug transport for a variety of biomedical applications [3–8]. PUs are usually synthesized using three components, for example, diols, diisocyanates, and chain extenders, and their properties can be modified either by changing the composition and nature of the diols, diisocyanates, and chain extenders or by incorporation of fillers in the polymer matrix [9]. Segmented PUs consist of hard and soft segment units that determine the mechanical properties of the polymer. Both relatively biostable and biodegradable PUs are used in different forms in artificial organs and medical devices [10]. Biodegradable PUs are used in drug delivery systems and implant materials for tissue repair [11].

Polymers with different forms of fillers such as carbon black, fullerenes, carbon nanotubes (CNTs), graphene, layered silicates (nanoclay), layered double hydroxides (LDHs), different metals, and ceramics are extensively used to modify the properties of pure polymers [12–17]. There are several metals and their oxides such as Ag, Au, TiO_2, Fe_3O_4, and ZnO that are frequently used to improve the properties of polymers. Since silver exhibits antibacterial properties, its nanoparticles embedded in polymers are utilized in various medical applications including wound dressings, artificial skin, bone tissue engineering, and urinary catheters [18–20]. Nanoparticles having superparamagnetic properties have received much attention as composites because they do not retain their magnetization properties in the absence of a magnetic field. This nanoparticle feature is very useful in magnetic resonance imaging and targeted drug delivery [21–24]. Fe_3O_4 is a superparamagnetic nanoparticle widely used in polymer composites due to its large surface area, biocompatibility, and nontoxic nature with good magnetic properties [25]. CNTs have also been used in composites due to their high electrical, thermal, and mechanical properties [26]. Inorganic materials having nanometer dimensions show very interesting physical and chemical properties, leading to development of new materials for various applications [27]. Montmorillonite (MMT), which is the major ingredient of bentonite, is commonly used for the

Advances in Polyurethane Biomaterials. http://dx.doi.org/10.1016/B978-0-08-100614-6.00006-8

preparation of polymer composites for enhancement of properties. In MMT, two tetrahedrally coordinated silicon atoms are joined to an edge-shared octahedral sheet of magnesium or aluminum hydroxide. Cationic species present in the lattice structure are replaceable by other cations, for example, Al^{3+} can be replaced by divalent species such as Fe^{2+} or Mg^{2+} and Mg^{2+} or even by monovalent Li^{1+}, leading to generation of a negative charge in the lattice that is counterbalanced by the positive ions present in the interlayer spacing. Due to the presence of weak van der Waals forces acting within the matrix, these materials can easily be dispersed and provide high surface areas available for interaction during synthesis. Another advantage of these nanoparticles is their easy surface modification through ion exchange, which can enhance their polymer compatibility. Considerable enhancements in the thermal stability [28–30], barrier properties [31–33], mechanical strength [34–36], elastic properties [37,38], biodegradation, and high energy shielding [39,40] were observed in nanocomposites using nanoclay as the filler [41]. Tuning of the morphology and mechanical properties of the polymer and its nanocomposites in the presence of nanoclay was also reported [9,42]. Nanoparticle-induced self-assembly in PUs has several benefits such as improvement in mechanical properties, thermal stability, and decrease of the rate of enzymatic degradation [43]. LDH and anionic clay have received much attention in the field of nanocomposites due to their anion exchange capabilities, catalysis, and delivery of drugs as well as biological molecules such as DNA and enzymes [44]. LDH has a brucite-like structure and the replacement of divalent cations by trivalent ones results in excess charges that are counterbalanced by anions located between two layers [45]. Enhancement in mechanical properties and thermal stability were observed in those polymer nanocomposites in which exfoliated/disordered LDH was used as filler material [46]. Recently, the use of carbon materials as a filler has received tremendous attention in the composite field due to their exceptional properties. Different forms of carbon allotropes are used and depending on their structure are termed as fullerenes (0-D), CNT and nanoribbons (1-D), graphene (2-D), and graphite (3-D). Fullerenes can be formed through wrapping of graphene sheets, which leads to the formation of CNT. Stacking of graphene sheets is responsible for the formation of the graphite allotrope of carbon [47]. Graphene, a single layer of sp^2 hybridized carbon atoms arranged in a hexagonal lattice, is the fundamental structural unit of all kinds of carbon allotropes [48]. The chemical modifications of graphene are comparatively simple and important properties such as mechanical, thermal, electronic, and optical can be varied [49–52]. This allows graphene to have a wide range of applications in the field of energy technology [53,54], sensors [55], nanoelectronics [56], composites [57–60], and biomaterials [61]. Zeolites, another inorganic material, are frequently used in nanocomposites and in catalysis. Zeolites are also used in various applications due to their mechanical and thermal stability [62]. Zeolites are aluminosilicate minerals containing micropores in their structure. Since aluminosilicates have a negatively charged oxygen framework, this excess charge is balanced by the positively charged cations. Zeolites can be utilized for the preparation of antibacterial polymer nanocomposites. By tuning the Si/Al ratio as well as ion exchange properties of zeolites, one can tune the properties of composites material for a variety of purposes [63]. Classification of nanoparticles with different dimensions are shown in Scheme 6.1.

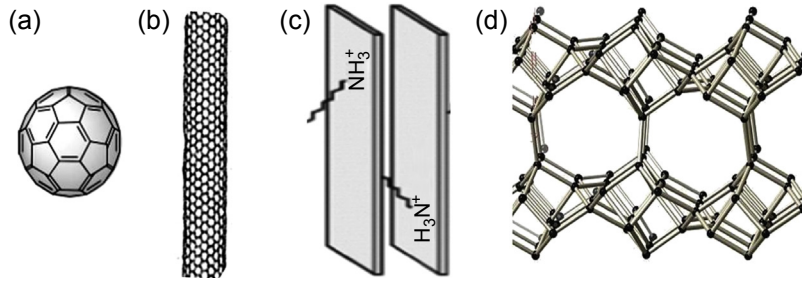

Scheme 6.1 Various types of nanoparticles. (a) 0D, fullerene; (b) 1D, carbon nanotube; (c) 2D, clay; and (d) 3D, zeolite [64–67].

6.2 Preparation of composites

There are different ways to prepare polymer composites and their advantages or drawbacks are as follows:

6.2.1 Solution casting technique

This is a common technique for the preparation of polymer composites. In the first step, dispersion of filler is achieved in appropriate solvent through mechanical stirring or sonication, followed by dissolution of the polymer in the same solvent. The dispersed fillers are then mixed with polymer solution either at room temperature or at higher temperature depending on the solubility of the polymer. Composite films are obtained either by precipitation or by casting the solution/mixture.

6.2.2 Melt blending process

This process of composite preparation is achieved using equipment such as an extruder [68] that has the ability to generate high shear force at elevated temperatures. The filler is added to the molten polymer and is sheared at a high rate. The advantage of this technique is that there is no solvent required. The drawbacks of this process are that a fine dispersion may not be achieved and that only limited filler concentrations can be used [69]. In addition the polymer chain may degrade under high shear conditions at high temperatures.

6.2.3 In Situ techniques

This is an efficient technique for the preparation of composites, allowing uniform dispersion of the filler to take place. Fillers are dispersed in monomer, possibly in the presence of solvent followed by the addition of the curing agents, hardener, or chain extender for polymerization at an appropriate temperature. One of the major advantages of this technique is that homogeneous dispersion of filler occurs in polymer matrix leading to significant improvement of most properties.

6.2.4 Latex method

Latex is a colloidal dispersion of polymer in an aqueous solvent. This method is more suitable for those polymers that can be prepared via emulsion polymerization or those that have the ability to form emulsion. It consists of an aqueous dispersion/stabilization of filler using a surfactant followed by the addition of the dispersed filler into the polymer latex. Nanocomposites can be obtained after freeze-drying the above mixture followed by melt processing. The latex method has several advantages including no requirement for organic solvent, reliability, ease of processing, and improved dispersion of the filler in the viscous polymer matrix [70].

6.3 Morphology

The presence of filler alters the morphology of the polymer matrix in various ways. Composite morphologies are highly influenced by the preparation method and extent and chemical nature of the filler used. Transmission electron microscopy (TEM), scanning electron microscopy (SEM) , atomic force microscopy (AFM), and optical microscopes are usually used to characterize the morphology. Dispersion of gold nanoparticles (0-D) in PU matrix is presented in Figure 6.1(a). At a low concentration, the distribution is homogeneous whereas it aggregates at a higher concentration (>65 ppm). The surface morphology observed through SEM shows a globular pattern in an Ag nanoparticle (AgNP) dispersed in a PU composite (Figure 6.1(a′)) while an AFM phase topography of the gold nanoparticles composite is given in Figure 6.1(a″). Roughness of the pure PU and its composites is in the range of 2.0–2.8 nm, indicating moderately flat surfaces. Hsu et al. and Cho were observed the formation of a lamellar structure through the hard segment of PU, which tends toward a micelle shape with increase of the hard segment content in PU [71,72]. Homogeneous dispersion of CNTs (1-D nanoparticles) in a PU matrix through *in situ* polymerization is shown in Figure 6.1(b) [73]. Uniform dispersion of filler through the *in situ* method provides a high surface area to interact better with polymer matrix and control the mechanical properties of the composite [74]. Better dispersion is also observed in the SEM and AFM images of the PU–CNT composites [75,76] (Figure 6.1(b′) and (b″)). The distribution of nanoclay (2-D nanoparticles) in a PU matrix and its effect on surface morphology are shown in Figure 6.1(c, c′, c″). Homogeneous dispersion is clearly observed as the composite was prepared *in situ* by dispersing nanoclay in polyol followed by polymerization with diol and diisocyanate. The surface morphology of the nanocomposite was also affected by the time of incorporation of the clay during the polymerization process. Pure PU exhibits a flake-like structure whereas the nanocomposites show a grainy morphology, which does not occur when the nanoclays are incorporated at an early stage of polymerization [9]. The banded pattern in the AFM image is evident in nanoclay PU composites with the band size becoming narrower in the composite than in pure PU. The SEM image of a PU–zeolite composite reveals the well-dispersed zeolite in the PU matrix (Figure 6.1(d)). The asymmetric structure of membrane consists of top skin, substructure, and bottom skin. Some aggregation of zeolite is observed in dense bottom skin. A study of the cross-section of the membrane reveals that the incorporation of zeolite is

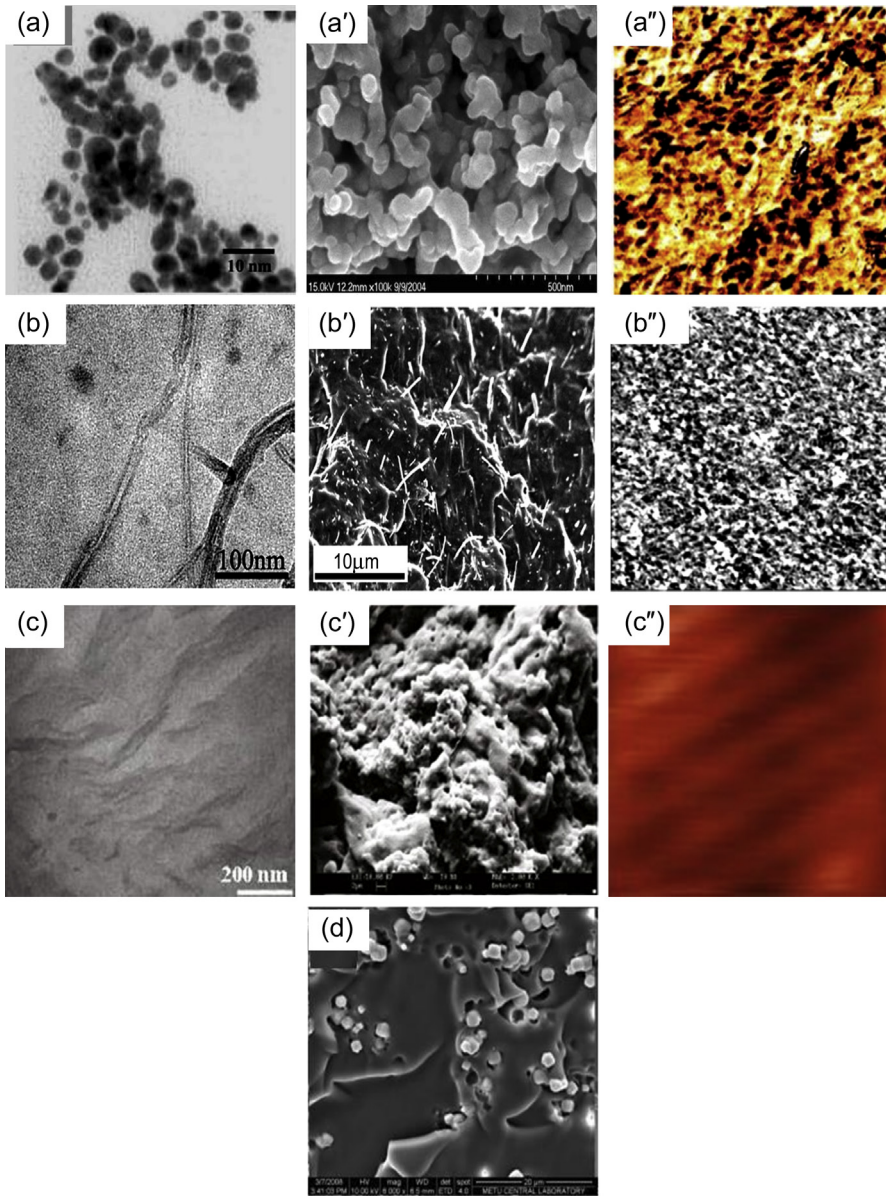

Figure 6.1 Morphology of polyurethane with various types of nanoparticles. (a) TEM micrograph of PU–Au nanocomposites containing 43.5 ppm gold particles [71], (a′) SEM image of PU–Ag fiber [72], (a″) AFM phase containing 17.4 ppm gold in PU matrix [71]; (b) TEM image of PU–CNT nanocomposites [73], (b′) SEM micrograph of PU–CNT nanocomposites containing 10 wt% CNT in matrix [75], (b″) AFM image of PU–MWCNTs [76]; (c)TEM image of PU–nanoclay, (c′) SEM micrograph of PU–nanoclay, and (c″) AFM image of PU–nanoclay [9]; and (d) SEM micrograph of PU–zeolite nanocomposites [78].

uniform only in the top skin (active layer) and in the substructure of the membrane. The pore size also decreases in the composite compared to the pure PU [77,78].

6.4 Structure

The incorporation of various nanoparticles in a PU matrix produces structural changes that are summarized here. X-ray diffraction (XRD) shows that the aromatic-based PU matrix is amorphous while the nano-TiO_2 (0-D filler) reveals its diffraction peaks (Figure 6.2(a)) [79]. The addition of CNT into a PU matrix disrupts the microphase morphology [80] (Figure 6.2(b)). Considerable enhancement of nanoclay interlayer spacing occurs when the clay is added to diol. Subsequent addition of diisocyanate and polymerization increase the spacing further as polymerization takes place, which displaces the silicate layers making an exfoliated structure [9] (Figure 6.2(c)). XRD patterns of PU–LDH nanocomposites exhibit the exfoliated nature at lower concentration of LDH while an intercalated nature is seen at higher LDH (2-D nanofiller) content [44]. PU having zeolite in its matrix shows a sharp peak at $2\theta = 37°$ and the intensity as well as position of this peak is affected by the content of the zeolite (Figure 6.2(d)) [81] due to the change in the

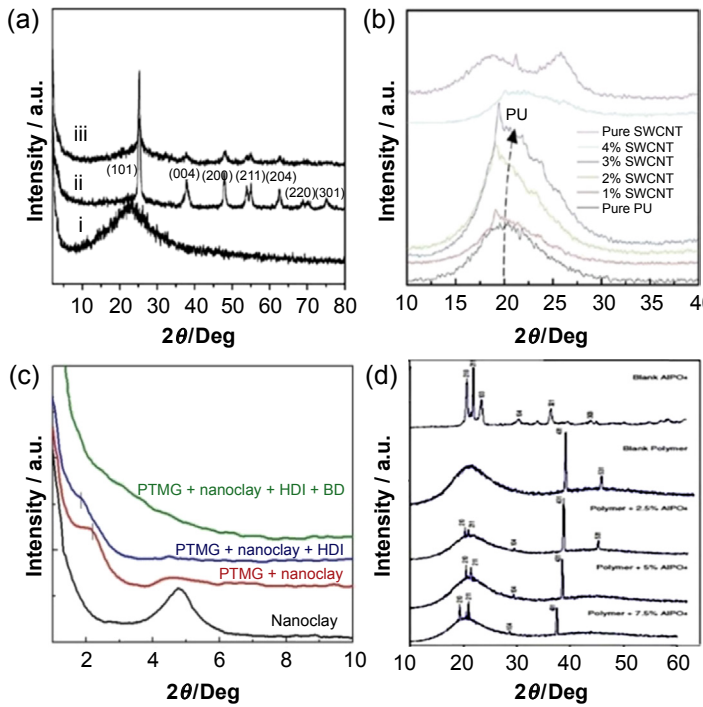

Figure 6.2 XRD patterns of PU and its nanocomposites with different types of nanoparticles: (a–i) pure PU, (a–ii) pure nano-TiO_2, and (a–iii) PU–nano-TiO_2 composite [79], (b) PU–CNT composites [80], (c) PU–clay nanocomposites [9], and (d) PU–$AlPO_4$-5 zeolite composites [81].

microcrystalline structure of the composites. For all types of filler, as expected, the intensity of the filler peak increases with increase of the content of filler in the composites.

6.5 Nanoparticle-induced self-assembly

Self-assembly plays an important role in enhancing the physical and mechanical properties of polymers. Nanoclay-induced self-assembly in aliphatic PUs via *in situ* polymerization has been observed [9]. Layer by layer self-assembly in aliphatic PU was observed through XRD, small-angle neutron scattering (SANS), AFM, and polarizing optical microscopy (POM). The appearance of a peak at ~5.8° (d-spacing ~1.6 nm) in XRD measurement suggests the formation of molecular layers in the PU nanocomposite (Figure 6.3(a)). Further, a shoulder/peak in SANS measurement with characteristic value ($\Lambda_c \sim 12$–14 nm) indicates the presence of a nanostructure in PU/nanocomposites (Figure 6.3(b)). The lower value of the characteristic length in nanocomposite (12 nm) compared to pure PU (14 nm) indicates nanoclay-induced self-assembly where a lesser number of molecular sheets is required for greater assembly

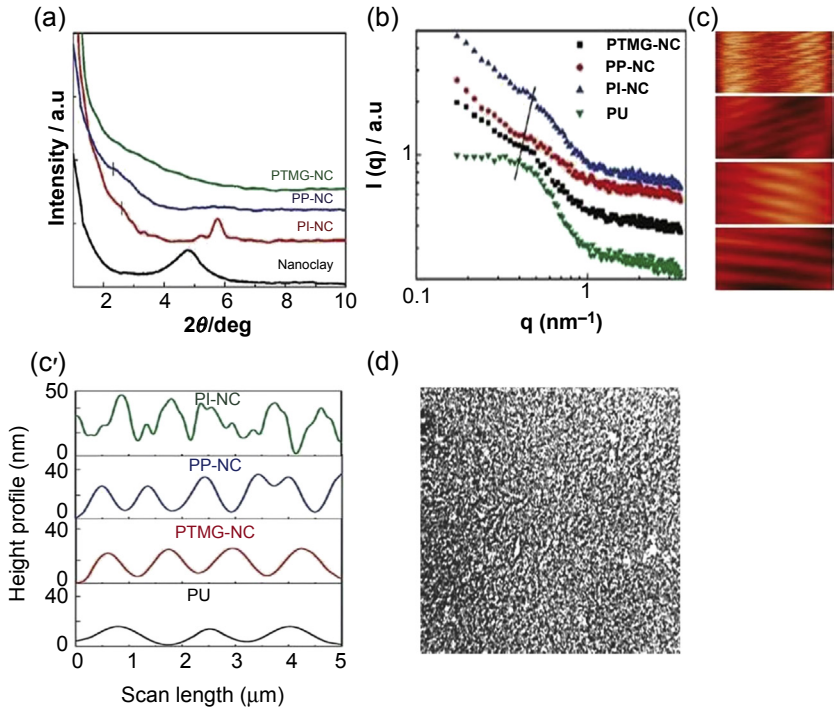

Figure 6.3 (a) X-ray diffraction patterns of organically modified Closite-30B nanoclay and nanocomposites, (b) small-angle neutron scattering patterns; I(q) versus q (wave vector) plot of indicated PU and nanocomposites, (c, c′) AFM image of PU and its nanocomposites with height profile, and (d) POM image PU–nanoclay composite [9].

through hydrogen bonding. The domain structure observed in AFM topographs suggests a larger assembly (lateral dimension of ~0.5 μm) (Figure 6.3(c)). A greater number of peaks as well as intensity of the height profile in the nanocomposite compared to pure PU appears in AFM topographs. This suggests the formation of a more consolidated structure in the nanocomposites. Larger structures in the nanocomposites were observed in the PU using optical microscopy (Figure 6.3(d)). The driving force for this self-assembly is the extensive hydrogen bonding between the urethane moieties in the polymer chains with the clay nanocrystals. Tuning of the surface morphology and properties due to the influence of clay through self-assembly was also revealed in aliphatic PUs having various chain extenders [42].

6.6 Mechanical behavior

The mechanical properties of composites depend on the amount, aspect ratio, surface area, orientation, interaction, and dispersion of the filler in polymer matrix [82]. Deka et al. synthesized PU nanocomposites with different weight percentages of Ag particles and measured the mechanical properties (tensile strength, bending, hardness (Shore A), and impact resistance). Tensile strength, hardness, and impact resistance increase with increasing weight percentage of nanoparticles while the elongation at break and bending remains the same compared to pure PU. The enhancement in mechanical properties was due to homogeneously dispersed Ag nanoparticles (AgNPs) with larger surface areas, which can interact with the matrix and facilitate easy transfer of stress to the fillers (Figure 6.4(a)) [83]. Mechanical properties of the composites can also be tuned by using different sizes of nanoparticles. Larger particles in the matrix result in lower stiffness and higher elongation at break compared to the composites with smaller particles, which show increased stiffness and lower elongation at break. Most differences in properties of the composites arise due to the interaction between filler and matrix polymer [84]. CNT with its high surface area and aspect ratio has a tensile strength of 50–200 GPa and Young's modulus of 1.2 TPa, which make it attractive for enhancing the mechanical properties of polymer matrices [68]. Figure 6.4(b) shows stress–strain curves of CNT-based PU composites as a function of CNT content [85]. The improvement of mechanical properties is due to the good dispersion of CNT that facilitates the load transfer between the polymer matrix and the CNTs. PU composites formed by using multiwall CNTs (MWNTs) and single wall CNTs (SWNTs) have shown different mechanical properties. MWNTs exhibit greater improvement in modulus whereas SWNT-based composites show improvement in tensile strength and elongation at break compared to the pure PU [86]. Considerable improvement in mechanical properties of PU/LDH composites is also reported. These improved properties are mainly due to the interaction of hydroxyl groups of LDH and the polar urethane linkages along with the high aspect ratio and orientation of LDH, which help the load transfer process during measurement (Figure 6.4(c)) [87]. PU/clay nanocomposites prepared through the *in situ* polymerization technique exhibit enhanced mechanical properties in terms of modulus and toughness. Orientation of the two-dimensional nanoclay toward the applied force field is responsible for the toughness enhancement in nanohybrids [88]. Incorporation

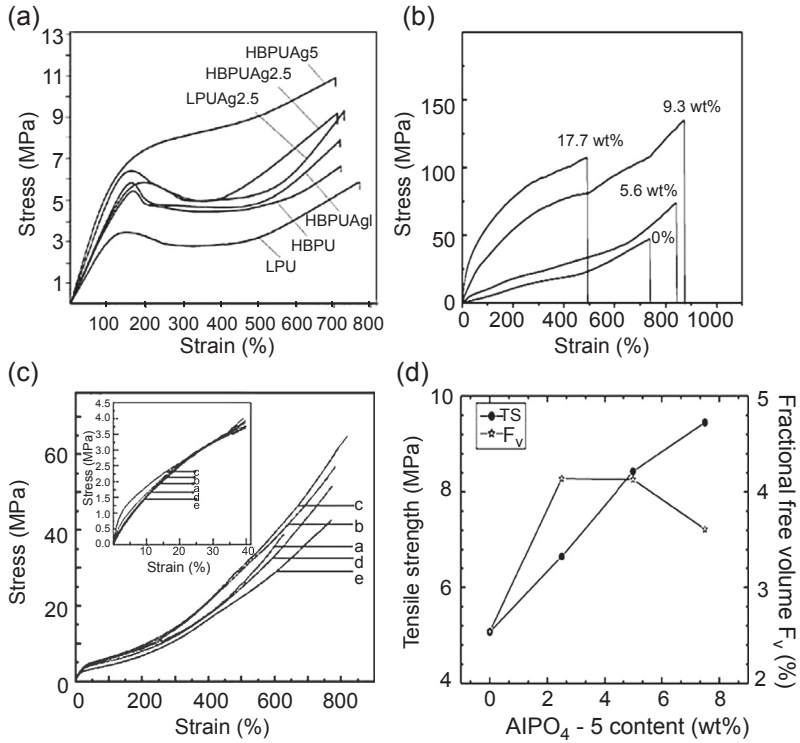

Figure 6.4 Mechanical behavior of polyurethane composites with various types of nanoparticles: (a) PU and its nanocomposites containing silver particles [83], (b) PU and its nanocomposites with CNTs [85], (c) PU–LDH nanocomposite (in which a, b, c, d, and e represent the pure PU, 1, 3, 5, and 8 wt% of LDH in matrix) [87], and (d) PU–zeolite composites [81].

of 2 wt% of graphene in PU matrix during the polymerization process increases tensile strength and elongation at break in PU/graphene composites presumably due to homogeneous dispersion of graphene in the PU matrix. TEM measurements suggest good interfacial interaction between the polymer chain and the graphene sheets [13]. Several workers report a decrease of mechanical properties of CNT PU nanocomposites due to poor dispersion of the CNTs and the preparation method (*ex situ* polymerization) [89,90]. The improvement in mechanical properties of TDI-based PUs after the addition of zeolites (*in situ* process) has been investigated by Kumar et al., comparing surface hardness, tensile strength, and modulus. Surface hardness of the composites increased slightly with the addition of zeolite $AlPO_4$-5. Considerable improvements in tensile strength and modulus were observed with increasing $AlPO_4$-5 content, which indicates good interfacial adhesion between the PU and the zeolite filler [81] (Figure 6.4(d)).

A general observation is that composites having smaller nanoparticles in a PU matrix exhibit higher storage modulus compared to larger particles. The larger surface area also causes a shifting of the damping factor (tan δ) peak toward higher temperatures compared to the pure PU [84] (Figure 6.5(a) and (b)). Incorporation of CNTs in a PU matrix leads

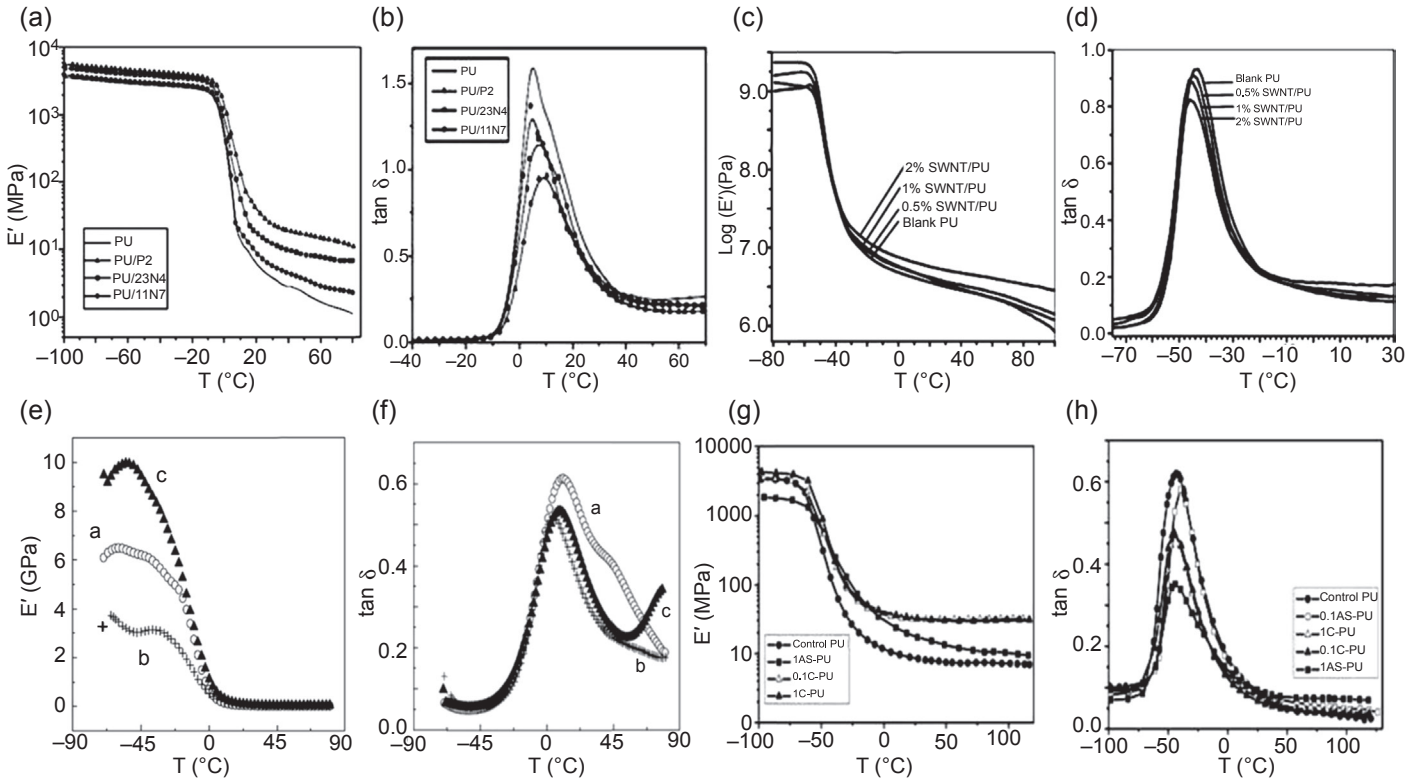

Figure 6.5 Dynamic mechanical behavior of polyurethane nanocomposite in the presence of various types of nanoparticles. (a and b) Storage modulus and damping factor in the presence of alumina [84], (c and d) storage modulus and damping factor in the presence of CNTs [86], (e and f) storage modulus and damping factor in the presence of clay [91], and (g and h) storage modulus and damping factor in the presence of zeolite, respectively [92].

to the enhancement in storage modulus at room temperature as well as a slight decrease in tan δ and glass transition temperature likely due to an increase in microphase separation creating slightly purer soft segment microdomains [86] (Figure 6.5(c) and (d)). The storage modulus and tan δ of nanoclay-based PU composites are presented in Figure 6.5(e) and (f). Different types of clay exhibit different behavior toward the storage modulus and damping behavior. Nanoclay with aromatic organic modification exhibits a higher storage modulus compared to the composites made of nanoclay modified with aliphatic ammonium salt. The peak position of tan δ curves of the composites shifted toward the lower temperature region and becomes narrower than that of the pure PU [91]. Composites of zeolite exhibit a different behavior of storage modulus in the glassy region. The calcined zeolite filler exhibits a higher storage modulus compared to freshly synthesized zeolite composites in the glassy region due to the increase in the density of material resulting from the loss of porosity after calcination. The addition of small amounts of as-prepared β-zeolite in the PU matrix shifts the damping peak toward higher temperatures due to restriction on the mobility of the polymer chains. However, as the content of filler increased, the peak shifts toward the lower temperature, a phenomenon not observed with the calcined zeolite [92] (Figure 6.5(g) and (h)).

The rheological behavior of PU-grafted SWCNT in terms of viscosity versus shear rate at 80 °C is presented in Figure 6.6(a). Grafted PU composites exhibit higher viscosity compared to the pure diol as well as the diol/SWCNT composites. The lowest shearing thinning exponent observed in grafted composites indicates better dispersion in polycaprolactone (PCL) diol [93]. The rheological behavior in terms of modulus and complex viscosity versus frequency of PU clay nanocomposites was studied by Mishra et al. [9]. Nanoclay-based composites exhibit higher storage modulus (G') and complex viscosity (η^*) compared to unfilled PU due to the presence of the nanoparticles. In the melt phase, the modulus drops abruptly at a certain frequency due to a disruption of the network structure. This disruptive frequency shifts toward higher frequency in the nanocomposites [9] (Figure 6.6(b) and (c)). Further increase of frequency enhances the storage modulus and complex viscosity.

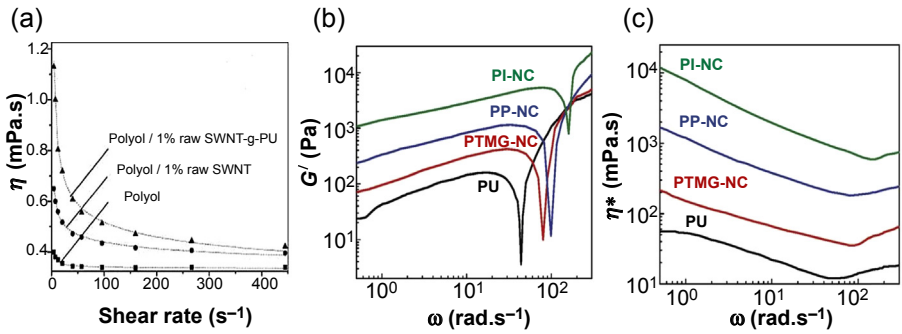

Figure 6.6 Rheological behavior of polyurethane and its nanocomposites in the presence of nanoparticles. (a) The viscosity at 80 °C versus shear rate for blank PCL diol and PCL diol/SWNT dispersions, (b) storage modulus, (c) complex viscosity of pure PU and its nanocomposites as a function of frequency at $T_{ref} = T_m + 20$ °C.

6.7 Thermal behavior

The thermal properties of a given composite are influenced, for example, by quality of dispersion, interaction with the polymer matrix, and filler content as well as the aspect ratio. Enhancement in the thermal stability was observed in composites by the addition of nano-TiO_2 in a PU matrix. The thermal degradation temperature increases from 347 to 365 °C in 1 wt% TiO_2 composites [94]. Composites having different particle dimensions exhibit a range of thermal stability [84] (Figure 6.7(a)). The addition of CNTs also affects the thermal stability of the composites. PU/CNT composites exhibit a two-step degradation process [95]. The addition of minute quantities of MWCNTs during the polymerization process of PU considerably enhances the thermal stability [96]. Figure 6.7(b) shows the thermogravimetric analysis (TGA) curves of PU/CNT

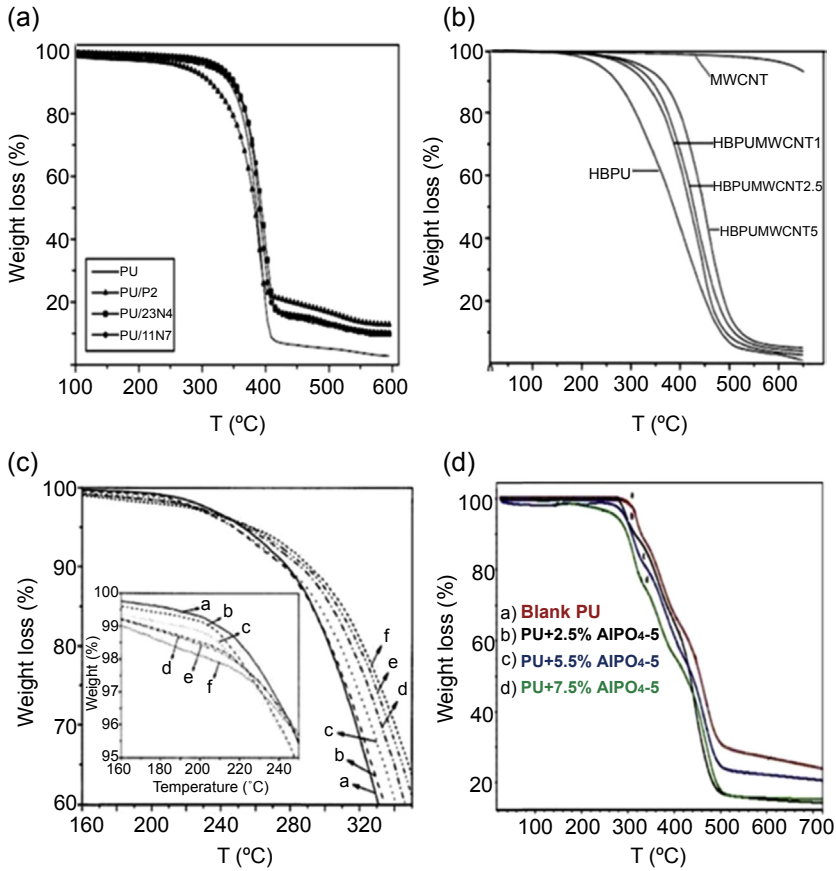

Figure 6.7 TGA curves of polyurethane and its nanocomposites in the presence of different types of nanoparticles. (a) In the presence of alumina powder [84], (b) in the presence of CNTs [96], (c) in the presence of clay (here a, b, c, d, e, and f represent 0, 1, 2, 3, 4, and 5 wt% of clay in PU matrix) [14], and (d) in the presence of zeolite [81].

composites. Incorporation of 1 wt% of MWCNTs in the PU matrix enhances the thermal degradation from 215 to 275 °C and the degradation temperature further increases with the increasing amounts of MWCNT in the PU matrix [97]. A comparison of the thermal stability of PU/CNT composites reveals that more stable dispersions result in better thermal stability [98]. LDH as a filler in PU matrix also enhances the thermal stability of the composites. Degradation patterns of the LDH composites were very similar to those of pure PU [44]. Similarly, composites of organically modified nanoclay–PU composites show better thermal stability than pure PU and the stability was further increased with nanoclay content due to the thermally insulating behavior of the nanoclay (Figure 6.7(c)) [14]. Different types of nanoclays exhibit a range of thermal stability. Nanocomposites having aromatic amine-modified clay exhibit better thermal stability than quaternary alkyl ammonium salt-containing nanocomposites [91]. Composites having graphene or modified graphene as filler exhibit better thermal stability than pure PU due to the tortuous path created by two-dimensional graphene sheets, which prevent the elimination of the volatile products along with the formation of char [99]. Incorporation of 2 wt% of graphene in PU matrix during the polymerization (*in situ*) leads to the improvement in thermal stability of 40 °C compared to the pure PU [13]. TGA of pure PU and its composites with zeolite 13X shows the effect of zeolite on thermal stability. The degradation temperature increases with increase of the zeolite content in composite, indicating good heat resistance and heat transfer properties of the zeolite filler (Figure 6.7(d)) [81,100]. CNTs exhibit thermal conductivity ~3000 W/m/K at room temperature and this property has been utilized to prepare thermally conductive composites [101]. Xia and Song observed a significant improvement of thermal conductivity of 21% and 42% for composites containing 1% of MWCTs and SWNTs, respectively [86]. Further increases of CNT reduce the thermal conductivity due to the large interfacial thermal resistance between the CNTs and the polymer matrix [102]. Similar results were also obtained in the case of MWNT/water-based PU composites prepared through the latex method [103].

Differential scanning calorimetry (DSC) thermograms of PU–Au nanocomposites are presented in Figure 6.8(a). Nanocomposites having 6.5×10^{-2} wt% gold particles in the matrix do not show an endothermic soft segment melting peak while composites with less than the amount of Au particles show a sharp melting endotherm. The disappearance of the peak at a higher content of Au particles is possibly due to gold–polyol interactions, which inhibit crystallization [104]. SWCNTs do not alter the glass transition temperature of composites of PCL-based PUs while the nanofiller strongly influences the melting behavior of the soft and hard segments. The melting temperatures of the soft and hard segments decrease slightly with increasing amounts of SWCNT (Figure 6.8(b)) [80]. In contrast the melting temperature of the soft segment increases in PU–nanoclay composites prepared through *in situ* polymerization where the nanoclay was incorporated before prepolymer formation. Interestingly a decrease in melting temperature is noted for the hard segment compared to the pure PU, indicating a strong interaction between the nanoclay and the hard segment of the aliphatic-based PU (Figure 6.8(c)). This suggests that the organically modified nanoclay disrupts the urethane interactions of the polymer chain, which causes a decrease in the melting temperature [9].

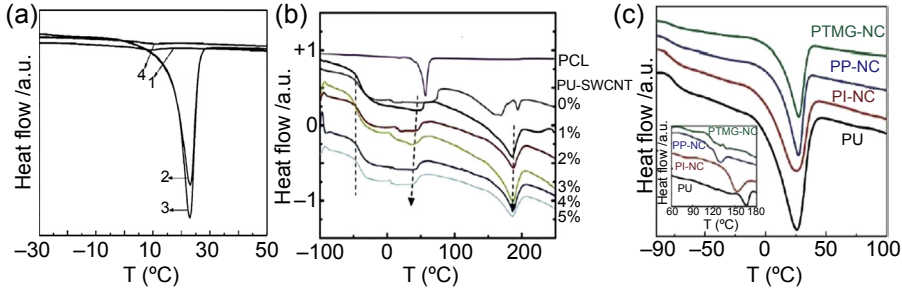

Figure 6.8 DSC curves of polyurethane and its nanocomposites in the presence of different types of nanoparticles. (a) PU–Au nanocomposites, 1 for pure PU, 2, 3, and 4 indicate 1.74, 4.35, and 6.5×10^{-2} wt% of Au nanoparticles [104], (b) PU–CNT composites [80], and (c) PU-nanoclay composites [9].

6.8 Flame retardancy

PUs can be used as coating materials for the improvement of flame retardant properties [105,106]. Initially, halogen and phosphorous-based materials were used in these applications [107]. Layer by layer nanocoating is an important process that can enhance the flame retardant activity of highly flammable materials like nylon [108], PET fabric [109], polycarbonate [110], and cotton [111,112]. PU coating with cationic boehmite and anionic vermiculite filler material exhibits considerable improvement in flame retardant activity. PU melts and ignites when a hand-held butane torch is focused on the uncoated PU sample for 10 s while a coated clay-filled PU is not influenced by the torch and retains its original shape [113]. Incorporation of a few percent of clay in a PU matrix enhances its the thermal stability and flame retardant properties due to the formation of a protecting clay layer on the polymer surface [114]. Patel and Patel have used different types of diisocyanate for the preparation of PU nanoclay composites and compared the flame retardant properties in terms of limiting oxygen index value. Nanocomposites show better flame retardant properties compared to the pure PU [115].

6.9 Antimicrobial activity

Nanoparticles, especially silver ions (Ag^+), are frequently used for their antibacterial activity. Ag^+ ions prevent the replication of the microbial DNA, which in turn suppress the expression of the ribosomal protein as well as the enzymes for ATP hydrolysis [116]. Liu et al. have prepared composites of MDI and H_{12}MDI-based PU using small, medium, and large sizes of silver nanoparticles to study the effect of nanoparticles size on bacterial activity (*Escherichia coli* and *Staphylococcus aureus*). The smaller size silver nanoparticles in composites show better response in comparison to the composites with larger particles [117]. PU composites using nanoscale silicate platelets (NSP) and AgNPs in different ratios also exhibit strong antibacterial activity. Figure 6.9 shows the bactericidal LIVE/DEAD analysis of the growth of *S. aureus* (after exposure for 12 h), indicating

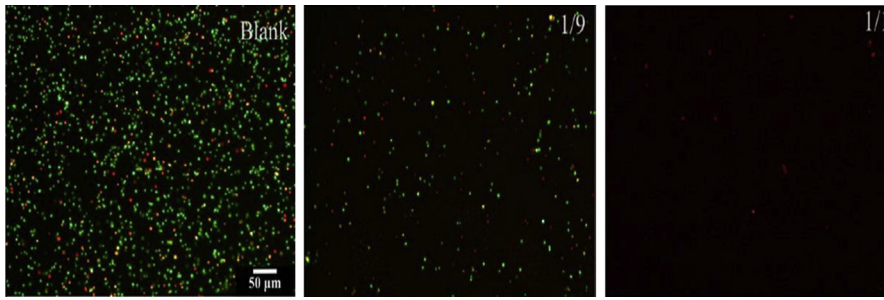

Figure 6.9 Bactericidal LIVE/DEAD analysis. Growth of *Staphylococcus aureus* (after 12 h exposure) on AgNP/NSP-PU-coated stainless steel. Greens are viable cells and reds are nonviable cells, where 1/1 and 1/9 are the ratios of AgNP/NSP in PU composites [118].

full inhibition for the composition of AgNP:NSP of 1:1 in a PU composite [118]. Zvekić et al. performed antimicrobial tests against bacteria and fungi (pour plate method) with nano-ZnO-containing PU varnishes. The colonies of *Pseudomonas aeruginosa* and *Saccharomyces cerevisiae* are not observed in the ZnO-containing varnishes in comparison to pure PU varnishes. Further, PU composites with 0.4 and 0.7 wt% ZnO inhibit growth of *S. aureus* by more than 85% and 95%, respectively [119].

6.10 Biomedical application of nanocomposites

6.10.1 Drug delivery

Controlled drug release and its application in the biomedical arena have received much attention from 1995 to 2015. Materials used as a vehicle for drug delivery should be safe, biocompatible, and nontoxic in nature and must not be the basis of an excess immune response. Other criteria such as suitable mechanical strength, easy processing/manufacturing, and a highly porous structure also must be met [120]. Large surface area along with the presence of different functionalities on the surface of CNTs provides an advantage for the loading of different kinds of drugs. Release of drug from polymer composites depends on several factors such as interactions between the drug and the polymer matrix, pH, and temperature of the medium [121]. Prolonged efficient drug release can also achieve a minimization of side effects [122]. Figure 6.10 shows the drug release profile of gentamicin sulfate in PU composites containing different types of nanoparticles. Albumin nanoparticle composites release drug at a faster rate in comparison to pure PU [123]. Similarly, CNT-based hyperbranched PU composites also exhibit slower release compared to pure PU and the release rate decreases with increasing amounts of CNTs in the matrix [124]. Two-dimensional nanoclay also sustained the release rate of drugs by controlling the diffusion mechanism through a tortuous path caused by the fine dispersion of the nanoclay in the PU matrix [42,125]. In summary, nanoparticles play an important role in drug release either by enhancing the interaction between the drug and the nanoparticles or by creating a tortuous diffusion path. Nanoparticles also appear to suppress the burst release of the drug from the PU.

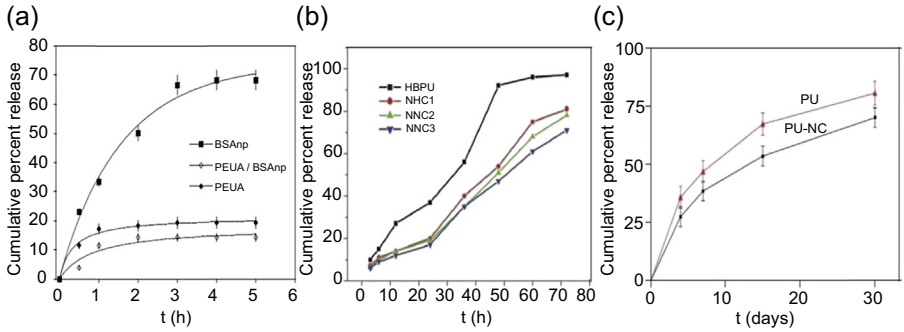

Figure 6.10 Sustained drug release profile of polyurethane composites with different types of nanoparticles. (a) In the presence of albumin nanoparticles [123], (b) in CNTs [124], the number indicates the percentage of CNT, and (c) in the presence of clay [125].

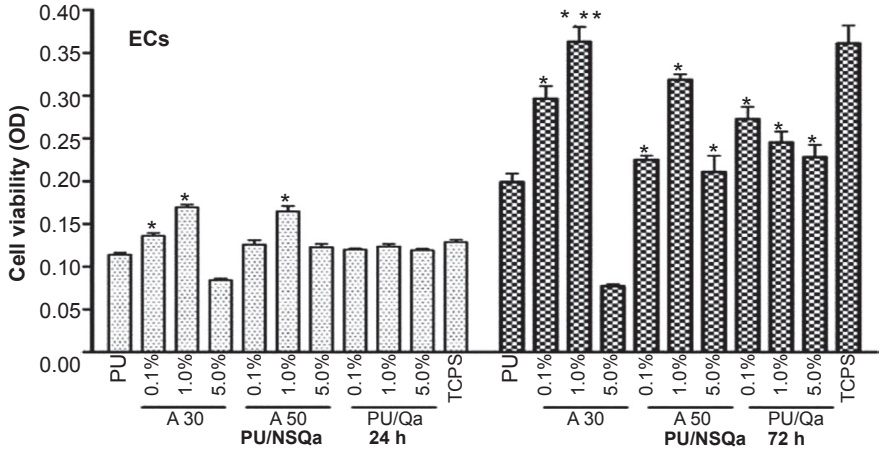

Figure 6.11 The viability of ECs grown on the surface of PU/NSQa (nanosilicate platelet exchange with cationic surfactant; A30 and A50; surfactant and reduced surfactant, respectively) and PU/Qa nanocomposites at 1 and 3 days. * indicates $P<0.05$, significantly greater than pure PU and ** indicates $P<0.05$, significantly greater than all other samples [129].

6.10.2 Tissue engineering

PUs have received considerable attention for engineering applications [126]. These include the construction of different types of structures for blood vessels, skin repair, and nerve reconstruction as well as bone growth [127]. Cell adhesion and proliferation on these structures are considered to be important in addition to their biocompatibility [128]. Different types of organically modified nanoclay have been used to prepare composites of PU for biological applications. Cell viability on composites was shown to be better than the PU matrix after 3 days of incubation [129] (Figure 6.11). Mishra et al. have also reported on the biocompatible nature of the PU/clay nanohybrid films in terms of cell viability, adhesion, and proliferation [9]. Recently, organically modified graphene has been used in tissue-engineering applications [130].

6.10.3 Implant materials

There are several polymers such as collagen, silicone rubber, and poly(tetrafluoroethylene) as well as PUs that are available for implant applications [131–133]. The basic requirement for implant material is that material should be mechanically strong to serve as a substrate for cell attachment and proliferation and be easily removable/bioadsorbable after the newly generated tissue restored the natural function [134]. Kannan et al. prepared PU (polycarbonate as soft segment) nanocomposites using polyhedral oligomeric silsesquioxanes (POSS) as the filler and used them as a biostable and biocompatible material [135]. POSS is responsible for the better resistance against oxidative and hydrolytic degradation for the PU–POSS composite [136]. The nanocomposite is nontoxic and has good thrombo-resistance and is also resistant toward degradation *in vivo*. *In vivo* experiments demonstrate minimal inflammation, capsule formation, and no degradation after 36 months of postimplantation in a sheep model compared to control [137]. Another *in vivo* study involving a vascular graft indicates good surface properties, superior biostability, and biocompatibility of the nanocomposite compared to the unfilled polymer [138]. Hence, a PU–POSS nanocomposite is an excellent material for tissue implants such as vascular grafts and heart valves. Khan et al. have prepared biocellulose nanoparticle-based composites (PU–BC) that have strong potential as bone tissue implants in terms of biodegradation, mechanical strength, porosity, and three-dimensional structure [139]. In summary, PU nanoparticles have potential in the biomedical arena for controlled drug delivery, tissue engineering, and implants and are a very active area of research.

6.11 Conclusions

Composites prepared using different types of nanoparticles can show superior properties compared to pure PU and have a wide range of applications in structural and biomedical fields. The surface morphology of nanocomposites is affected by the nature and amount of the nanoparticles embedded in polymer matrix. Different shapes and sizes of the nanoparticles play a significant role in enhancement of the mechanical, rheological, thermal, and fire retardant properties of the PU nanocomposites. Considerable improvements in antibacterial properties have been reported using nanocomposites compared to pure PU. Incorporation of the different kinds of nanoparticles in PU matrix alters the biocompatible nature of the composites, suggesting that PU composites may have use in biomaterial applications.

Acknowledgments

The author (D.K. Patel) gratefully acknowledges the financial support from Council for Scientific and Industrial Research (CSIR-UGC), New Delhi, in the form of a fellowship. The authors also acknowledge the receipt of research funding from Council for Scientific and Industrial Research (CSIR), New Delhi, Government of India (Project No. 02(0074)/12/EMR-II).

References

[1] Lan PN, Corneillie S, Schacht E, Davies M, Shard A. Synthesis and characterization of segmented polyurethanes based on amphiphilic polyester diols. Biomaterials December 1996;17(23):2273–80.
[2] Guan J, Fujimoto KL, Sacks MS, Wanger WR. Preparation and characterization of highly porous, biodegradable polyurethane scaffolds for soft tissue applications. Biomaterials June 2005;26(18):3961–71.
[3] Lee SH, Cyriac A, Jeon JY, Lee BY. Preparation of thermoplastic polyurethanes using in situ generated poly (propylene carbonate)-diols. Polym Chem March 2012;3(3):1215.
[4] Cyriac A, Lee SH, Lee BY, et al. Preparation of flame retarding poly (propylene carbonates). Green Chem October 2011;13(13):3469–75.
[5] Xu H, Chang J, Chen Y, Fan H, Shi B. Asymmetric polyurethane membrane with inflammation-responsive antibacterial activity for potential wound dressing application. J Mater Sci October 2013;48(19):6625–39.
[6] Camposa E, Cordeiroa R, Santosb AC, Gil MH, et al. Design and characterization of bi-soft segmented polyurethane microparticles for biomedical application. Colloids Surf B Biointerfaces July 2011;88:477–82.
[7] Molak ID, Lekka M, Kurzydlowski KJ. Surface properties of polyurethane composites for biomedical applications. Appl Surf Sci April 2013;270:553–60.
[8] Choi Y, Nirmala R, Lee JY, Rahman M, Hong ST, Kim HY. Antibacterial ciprofloxacin HCl incorporated polyurethane composite nanofibers via electrospinning for biomedical applications. Ceram Int July 2013;39(5):4937–44.
[9] Mishra A, Purkayastha BPD, Roy JK, Aswal VK, Maiti P. Tunable properties of self-assembled polyurethane using two–dimensional nanoparticles: potential nano-biohybrid. Macromolecules November 2010;43:9928–36.
[10] Zdrahala RJ, Zdrahala IJ. Biomedical applications of polyurethanes: a review of past promises, present realities, and a vibrant future. J Biomater Appl July 1999;14(1):67–90.
[11] Sun X, Gao H, Wu G, Wang Y, Fan Y, Ma J. Biodegradable and temperature-responsive polyurethane for adriamycin delivery. Int J Pharm June 2011;412:52–8.
[12] Li F, Qi L, Yang J, Xu M, Luo X, Ma D. Polyurethane/conducting carbon black composites: structure, electric conductivity, strain recovery behavior, and their relationships. J Appl Polym Sci January 2000;75:68–77.
[13] Wang X, Hu Y, Song L, Yang H, Xing W, Lu H. *In situ* polymerization of graphene nanosheets and polyurethane with enhanced mechanical and thermal properties. J Mater Chem February 2011;21:4222–7.
[14] Lee HT, Lin LH. Waterborne polyurethane/clay nanocomposites: novel effect of the clay and its interlayer ions on the morphology and physical and electrical properties. Macromolecules August 2006;39(18):6133–41.
[15] Wang Q, O'Hare D. Recent advances in the synthesis and application of layered double hydroxide (LDH) nanosheets. Chem Rev March 2012;112(7):4124–55.
[16] Bigg DM. Mechanical, thermal, and electrical properties of metal fiber-filled polymer composites. Polym Eng Sci December 1979;19(16):1188–92.
[17] Arbatti M, Shan X, Cheng ZY. Ceramic–polymer composites with high dielectric constant. Adv Mater May 2007;19(10):1369–72.
[18] Saint S, Elmore JG, Koepsell TD, et al. The efficacy of silver alloy-coated urinary catheters in preventing urinary tract infection: a meta-analysis. Am J Med September 1998;05:236–41.

[19] Bishop JB, Phillips LG, Mustoe TA. A prospective randomized evaluator-blinded trial of two potential wound healing agents for the treatment of venous stasis ulcers. J Vasc Surg August 1992;16:251–7.
[20] Morones JR, Elechiguerra JL, Camacho A, et al. The bactericidal effect of silver nanoparticles. Nanotechnology August 2005;16:2346–53.
[21] Sitharaman B, Kissell KR, Rusakova I, et al. Superparamagnetic gadonanotubes are high-performance MRI contrast agents. Chem Commun July 2005;31:3915–7.
[22] Cho HS, Dong ZY, Gu HC, et al. Fluorescent, superparamagnetic nanospheres for drug storage, targeting, and imaging: a multifunctional nanocarrier system for cancer diagnosis and treatment. ACS Nano September 2010;4:5398–404.
[23] Zhao Y, Lu Y, Lin LN, et al. Synthesis of superparamagnetic $CaCO_3$ mesocrystals for multistage delivery in cancer therapy. Small November 2010;6:2436–42.
[24] Huang YJ, Liu MZ, Gong QY, et al. A novel magnetic triple-responsive composite semi-IPN hydrogels for targeted and controlled drug delivery. Eur Polym J October 2012;48:1734–44.
[25] Gupta AK, Gupta M. Synthesis and surface engineering of iron oxide nanoparticles for biomedical applications. Biomaterials June 2005;26:3995–4021.
[26] Baughman RH, Zakhidov AA, Heer WAD. Carbon nanotubes-the route toward applications. Science August 2002;297:787–92.
[27] Schubert U. Polymers reinforced by covalently bonded inorganic clusters. Chem Mater June 2001;13:3487–94.
[28] Gorrasi G, Tortora M, Vittoria V. Synthesis and physical properties of layered silicates/polyurethane nanocomposites. J Polym Sci Part B Polym Phys July 2005;43:2454–67.
[29] Devaux E, Rochery M, Bourbigot S. Polyurethane/clay and polyurethane/POSS nanocomposites as flame retarded coating for polyester and cotton fabrics. Fire Mater December 2002;26:149–54.
[30] Solarski S, Benali S, Rochery M, Devaux E, Alexandre M, Monteverde F, et al. Synthesis of a polyurethane/clay nanocomposite used as coating: interactions between the counterions of clay and the isocyanate and incidence on the nanocomposite structure. J Appl Polym Sci November 2005;95:238–44.
[31] Xu R, Manias E, Snyder AJ. New biomedical poly(urethane urea)- layered silicate nanocomposites. Macromolecules December 2001;34:337–9.
[32] Osman MA, Mittal V, Morbidelli M, Suter UW. Polyurethane adhesive nanocomposites as gas permeation barrier. Macromolecules December 2003;36:9851–8.
[33] Jana KK, Charan C, Shahi VK, Mitra K, Ray B, Rana D, et al. Functionalized poly-(vinylidene fluoride) nanohybrid for superior fuel cell membrane. J Membr Sci February 2015;481:124–36.
[34] Beloqui BJ, Garcia JCF, Martinez JMM, et al. Rheological properties of thermoplastic polyurethane adhesive solutions containing fumed silicas of different surface areas. Int J Adhes Adhes August 1999;19:321–8.
[35] Yao KJ, Song M, Hourston DJ, Luo DZ. Polymer/layered clay nanocomposites: 2 polyurethane nanocomposites. Polymer November 2002;43:1017–20.
[36] Ma J, Zhang S, Qi Z. Synthesis and characterization of elastomeric polyurethane/clay nanocomposites. J Appl Polym Sci August 2001;82:1444–8.
[37] Chen TK, Tien YI, Wei KH. Synthesis and characterization of novel segmented polyurethane/clay nanocomposite via poly(ε-caprolactone)/clay. J Polym Sci Part A Polym Chem July 1999;37:2225–33.
[38] Petrovic ZS, Javni I, Waddon A, Banhegyi G. Structure and properties of polyurethane–silica nanocomposites. J Appl Polym Sci April 2000;76:133–51.

[39] Singh NK, Singh SK, Dash D, Purkayastha BPD, Roy JK, Maiti P. Nanostructure controlled anti-cancer drug delivery using poly(3-caprolactone) based nanohybrids. J Mater Chem 2012;22:17853–63.
[40] Tiwari VK, Kulriya PK, Avasthi DK, Maiti P. Radiation-resistant behavior of poly-(vinylidene fluoride)/layered silicate nanocomposites. ACS Appl Mater Interfaces December 2009;1(2):311–8.
[41] Discher BM, Won YY, Ede DS, Hammer DA, et al. Polymersomes: tough vesicles made from diblock copolymers. Science May 1999;284:1143–6.
[42] Mishra A, Purkayastha BPD, Roy JK, Aswal VK, Maiti P. Nanoparticle controlled self-assembly in varying chain extended polyurethanes as potential nanobiomaterials. J Phys Chem C December 2012;116:2260–70.
[43] Choy JH, Kwak SY, Park JS, Portier J. Intercalative nanohybrids of nucleoside monophosphates and DNA in layered metal hydroxide. J Am Chem Soc May 1999;121:1399–400.
[44] Guo S, Zhang C, Peng H, Wang W, Liu T. Structural characterization, thermal and mechanical properties of polyurethane/CoAl layered double hydroxide nanocomposites prepared via in situ polymerization. Compos Sci Technol February 2011;71:791–6.
[45] Chen W, Qu B. LLDPE/ZnAl LDH-exfoliated nanocomposites: effects of nanolayers on thermal and mechanical properties. J Mater Chem May 2004;14:1705–10.
[46] Kim H, Abdala AA, Macosko CW. Graphene/polymer nanocomposites. Macromolecules July 2010;43:6515–30.
[47] Terrones M, Olga Martín O, Cabanelas JC, Baselga J. Interphases in graphene polymer-based nanocomposites: achievements and challenges. Adv Mater September 2011;23:5302–10.
[48] Novoselov KS, Geim AK, Morozov SV, et al. Electric field effect in atomically thin carbon films. Science October 2004;306:666–9.
[49] Zhang K, Zhang LL, Zhao XS, et al. Graphene-polyaniline nanofiber composites as supercapacitor electrodes. Chem Mater January 2010;22:1392–401.
[50] Balandin AA, Ghosh S, Bao WZ, et al. Superior thermal conductivity of single-layer graphene. Nano Lett February 2008;8:902–7.
[51] Latil S, Henrard L. Charge carriers in few-layer graphene films. Phys Rev Lett July 2006;97:036803–6.
[52] Stoller MD, Park S, Zhu YW, et al. Graphene-based ultracapacitors. Nano Lett September 2008;8:3498–502.
[53] Wang L, Lee K, Sun YY, et al. Graphene oxide as an ideal substrate for hydrogen storage. ACS Nano September 2009;3:2995–3000.
[54] Lu CH, Yang HH, Zhu CL, et al. A graphene platform for sensing biomolecules. Angew Chem Int Ed May 2009;121:4879–81.
[55] Xuan Y, Wu YQ, Shen T, et al. Atomic-layer-deposited nanostructures for graphene-based nanoelectronics. Appl Phys Lett January 2008;92:013101–3.
[56] Yang XM, Tu YF, Li L, et al. Well-dispersed chitosan/graphene oxide nanocomposites. ACS Appl Mater Interfaces June 2010;2:1707–13.
[57] Bai H, Li C, Wang XL, et al. A pH-sensitive graphene oxide composite hydrogel. Chem Commun March 2010;46:2376–8.
[58] Sun ST, Wu PY. A one-step strategy for thermal- and pH-responsive graphene oxide interpenetrating polymer hydrogel networks. J Mater Chem February 2011;21:4095–7.
[59] Fang F, Long J, Zhao WF, et al. pH-Responsive chitosan-mediated graphene dispersions. Langmuir October 2010;26:16771–4.
[60] Liu Z, Robinson JT, Sun XM, et al. PEGylated nanographene oxide for delivery of water-insoluble cancer drugs. J Am Chem Soc July 2008;130:10876–7.

[61] Jia M, Peinemann KV, Behling RD. preparation and characterization of thin film zeolite–pdms composite membranes. J Membr Sci October 1992;73:119–28.
[62] Berry MB, Libby BE, Rose K, Haas KH, Thompson RW. Incorporation of zeolites into composite matrices. Microporous Mesoporous Mater 2000;39:205–17.
[63] Aksoy EA, Akata B, Bac N, Hasirci N. Preparation and characterization of zeolite beta–polyurethane composite membranes. J Appl Polym Sci June 2007;104(5):3378–87.
[64] Giacalone F, Martin N. Fullerene polymers: synthesis and properties. Chem Rev December 2006;106:5136–90.
[65] Bianco A, Kostarelos K, Partidos CD, Prato M. Biomedical applications of functionalised carbon nanotubes. Chem Commun February 2005;5:571–7.
[66] Ouros ACD, Souzab MOD, Pastore HO. Metallocene supported on inorganic solid supports: an unfinished history. J Braz Chem Soc 2014;25(12):2164–85.
[67] Wang YX, Gies H, Marler B. Synthesis and crystal structure of zeolite RUB-41 obtained as calcination product of a layered precursor: a systematic approach to a new synthesis route. Chem Mater December 2005;17:43–9.
[68] Ma PC, Siddiqui NA, Marom G, Kim JK. Dispersion and functionalization of carbon nanotubes for polymer-based nanocomposites: a review. Composites Part A October 2010;41(10):1345–67.
[69] Moniruzzaman M, Winey KI. Polymer nanocomposites containing carbon nanotubes. Macromolecules July 2006;39:5194–205.
[70] Grossiord N, Loos J, Regev O, Koning CE. Toolbox for dispersing carbon nanotubes into polymers to get conductive nanocomposites. Chem Mater January 2006;18(5):1089–99.
[71] Hsu SH, Tang CM, Tseng HJ. Gold nanoparticles induce surface morphological transformation in polyurethane and affect the cellular response. Biomacromolecules December 2008;9(1):241–8.
[72] Cho JW, So JH. Polyurethane–silver fibers prepared by infiltration and reduction of silver nitrate. Mater Lett February 2006;60:2653–6.
[73] Xiong J, Zheng Z, Qin X, Li M, Li H, Wang X. The thermal and mechanical properties of a polyurethane/multi-walled carbon nanotube composite. Carbon May 2006;44:2701–7.
[74] Liu LQ, Wagner HD. Rubbery and glassy epoxy resins reinforced with carbon nanotubes. Compos Sci Technol September 2005;65:1861–8.
[75] Koerner H, Liu W, Alexander M, Mirau P, Vaia RA, et al. Deformation–morphology correlations in electrically conductive carbon nanotube—thermoplastic polyurethane nanocomposites. Polym J March 2005;46:4405–20.
[76] Yoo HJ, Jung YC, Sahoo NG, Cho JW. Polyurethane-carbon nanotube nanocomposites prepared by in-situ polymerization with electroactive shape memory. J Macromol Sci Part B Phys August 2006;45:441–51.
[77] Ciobanu G, Carja G, Ciobanu O. Structure of mixed matrix membranes made with SAPO-5 zeolite in polyurethane matrix. Microporous Mesoporous Mater February 2008;115:61–6.
[78] Kamisoglu K, Aksoy EA, Akata B, Hasirci N, Bac N. Preparation and characterization of antibacterial zeolite–polyurethane composites. J Appl Polym Sci September 2008;110:2854–61.
[79] Chen J, Zhou Y, Nan Q, Sun Y, Ye X, Wang Z. Synthesis, characterization and infrared emissivity study of polyurethane/TiO_2 nanocomposites. Appl Surf Sci May 2007;253:9154–8.
[80] Lee HF, Yu HH. Study of electroactive shape memory polyurethane–carbon nanotube hybrids. Soft Matter February 2011;7:3801–7.
[81] Kumar BVS, Siddaramaiah, Shayan MB, Byrappa K, et al. Effect of zeolite particulate filler on the properties of polyurethane composites. J Polym Res May 2010;17:135–42.
[82] Kim JK, Mai Y. Engineered interfaces in fiber reinforced composites. Oxford: Elsevier; 1998. p. 1–100.

[83] Deka H, Karak N, Kalita RD, Buragohain AK. Bio-based thermostable, biodegradable and biocompatible hyperbranched polyurethane/Ag nanocomposites with antimicrobial activity. Polym Degrad Stab June 2010;95:1509–17.
[84] Gatos KG, Alcazar JGM, Psarras GC, Thomann R, Kocsis JK. Polyurethane latex/water dispersible boehmite alumina nanocomposites: thermal, mechanical and dielectrical properties. Compos Sci Technol September 2007;67:157–67.
[85] Chen W, Tao X, Liu Y. Carbon nanotube-reinforced polyurethane composite fibers. Compos Sci Technol March 2006;66:3029–34.
[86] Xia H, Song M. Preparation and characterization of polyurethane–carbon nanotube composites. Soft Matter October 2005;1:386–94.
[87] Kotal M, Kuila T, Srivastava SK, Bhowmick AK. Synthesis and characterization of polyurethane/Mg-Al layered double hydroxide nanocomposites. J Appl Polym Sci July 2009;114:2691–9.
[88] Shah D, Maiti P, Gunn E, Schmidt DF, Jiang DD, Batt CA, et al. Dramatic enhancements in toughness of polyvinylidene fluoride nanocomposites via nanoclay-directed crystal structure and morphology. Adv Mater August 2004;16:1173–7.
[89] Ma PC, Tang BZ, Kim JK. Effect of CNT decoration with silver nanoparticles on electrical conductivity of CNT–polymer composites. Carbon September 2008;46(11):1497–505.
[90] Ma PC, Liu MY, Kim JK, Tang BZ, et al. Enhanced electrical conductivity of nanocomposites containing hybrid fillers of carbon nanotubes and carbon black. ACS Appl Mater Interfaces May 2009;1(5):1090–6.
[91] Xiong J, Liu Y, Yang X, Wang X. Thermal and mechanical properties of polyurethane/montmorillonite nanocomposites based on a novel reactive modifier. Polym Degrad Stab December 2004;86(3):549–55.
[92] Aksoy EA, Akata B, Bac N, Hasirc N. Preparation and characterization of zeolite beta–polyurethane composite membranes. J Appl Polym Sci March 2007;104:3378–87.
[93] Xia H, Song M. Preparation and characterisation of polyurethane grafted single-walled carbon nanotubes and derived polyurethane nanocomposites. J Mater Chem March 2006; 16:1843–51.
[94] Saha MC, Kabir MdE, Jeelani S. Enhancement in thermal and mechanical properties of polyurethane foam infused with nanoparticles. Mater Sci Eng A April 2008;479:213–22.
[95] Rana S, Karak N, Cho JW, Kim YH. Enhanced dispersion of carbon nanotubes in hyperbranched polyurethane and properties of nanocomposites. Nanotechnology November 2008;19:495707 (8 pp.).
[96] Deka H, Karak N, Kalita RD, Buragohain AK. Biocompatible hyperbranched polyurethane/multi-walled carbon nanotube composites as shape memory materials. Carbon February 2010;4(8):2013–22.
[97] Jin SH, Park YB, Yoon KH. Rheological and mechanical properties of surface modified multi-walled carbon nanotube-filled PET composite. Compos Sci Technol December 2007;67:3434–41.
[98] Jana RN, Cho JW. Thermal stability and molecular interaction of polyurethane nanocomposites prepared by in situ polymerization with functionalized multiwalled carbon nanotubes. J Appl Polym Sci June 2008;108:2857–64.
[99] Cao Y, Feng J, Wu P. Preparation of organically dispersible graphene nanosheet powders through a lyophilization method and their poly(lactic acid) composites. Carbon June 2010;48:3834–9.
[100] Lv Z, Zhang L, Yang Y, Bi X. Preparation and properties of polyurethane/zeolite 13X composites. Mater Des June 2011;32:3624–8.
[101] Smalla JP, Shib L, Kima P. Mesoscopic thermal and thermoelectric measurements of individual carbon nanotubes. Solid State Commun 2003;127(2):181–6.

[102] Huxtable ST, Cahill DG, Shenogin S, Keblinski P, et al. Interfacial heat flow in carbon nanotube suspensions. Nat Mater October 2003;2:731–4.
[103] Cai D, Song M. Latex technology as a simple route to improve the thermal conductivity of a carbon nanotube/polymer composite. Carbon September 2008;46:2107–12.
[104] Hsu SH, Chou CW, Tseng SM. Enhanced thermal and mechanical properties in polyurethane/Au nanocomposites. Macromol Mater Eng December 2004;289:1096–101.
[105] Morgan AB. Flame retarded polymer layered silicate nanocomposites: a review of commercial and open literature systems. Polym Adv Technol April 2006;17(4):206–17.
[106] Zhu SW, Shi WF. Synthesis and photopolymerization of hyperbranched polyurethane acrylates applied to UV curable flame retardant coatings. Polym Int March 2002;51(3):223–7.
[107] Yuan CY, Chen SY, Tsai CH, Chiu YS, Chen-yang YW. Thermally stable and flame-retardant aromatic phosphate and cyclotriphosphazene-containing polyurethanes: synthesis and properties. Polym Adv Technol May 2005;16(5):393–9.
[108] Apaydin K, Laachachi A, Ball V, Jimenez M, Ruch D, et al. Polyallylamine–montmorillonite as super flame retardant coating assemblies by layer-by layer deposition on polyamide. Polym Degrad Stab November 2013;98:627–34.
[109] Carosio F, Laufer G, Alongi J, Camino G, Grunlan JC. Layer-by-layer assembly of silica-based flame retardant thin film on PET fabric. Polym Degrad Stab May 2011;96:745–50.
[110] Carosio F, Blasio AD, Alongi J, Malucelli G. Layer by layer nanoarchitectures for the surface protection of polycarbonate. Eur Polym J February 2013;49(2):397–404.
[111] Li YC, Mannen S, Morgan AB, Chang S, Yang YH, Condon B, et al. Intumescent all-polymer multilayer nanocoating capable of extinguishing flame on fabric. Adv Mater September 2011;23(34):3926–31.
[112] Huang G, Yang J, Gao J, Wang X. Thin films of intumescent flame retardant-polyacrylamide and exfoliated graphene oxide fabricated via layer-by-layer assembly for improving flame retardant properties of cotton fabric. Ind Eng Chem Res September 2012;51:12355–66.
[113] Patra D, Vangal P, Cain AA, Cho C, Regev O, Grunlan JC. Inorganic nanoparticle thin film that suppresses flammability of polyurethane with only a single electrostatically-assembled bilayer. ACS Appl Mater Interfaces September 2014;6:16903–8.
[114] Wang ZY, Han EH, Ke W. Fire-resistant effect of nanoclay on intumescent nanocomposite coatings. J Appl Polym Sci February 2007;103(3):1681–9.
[115] Patel RH, Patel KS. Synthesis of flame retardant polyester-urethanes and their applications in nanoclay composites and coatings. Polym Int March 2014;63(3):529–36.
[116] Shah MdSAS, Nag M, Kalagara T, Singh S, Manorama SV. Silver on PEG-PU-TiO_2 polymer nanocomposite films: an excellent system for antibacterial applications. Chem Mater March 2008;20:2455–60.
[117] Liu HL, Dai SA, Fu KY, et al. Antibacterial properties of silver nanoparticles in three different sizes and their nanocomposites with a new waterborne polyurethane. Int J Nanomedicine November 2010;2010:1017–28.
[118] Huang YH, Chen MHH, Lee BH, Hsieh KH, Chang CH, et al. Evenly distributed thin-film Ag coating on stainless plate by tricomponent Ag/silicate/PU with antimicrobial and biocompatible properties. ACS Appl Mater Interfaces October 2014;6:20324–33.
[119] Zvekic D, Srdic VV, Karaman MA, Matavulj MN. Antimicrobial properties of ZnO nanoparticles incorporated in polyurethane varnish. Process Appl Ceram 2011;5(1):41–5.
[120] Papkov MS, Agashi K, Olaye A, Shakesheff K, Domb AJ. Polymer carriers for drug delivery in tissue engineering. Adv Drug Deliv Rev May 2007;59:187–206.
[121] Rosenbauer EM, Wagner M, Musyanovych A, Landfester K. Controlled release from polyurethane nanocapsules via pH- UV-light- or temperature-induced stimuli. Macromolecules May 2010;43:5083–93.

[122] Cho K, Wang X, Nie S, Chen ZG, Shin DM. Therapeutic nanoparticles for drug delivery in cancer. Clin Cancer Res March 2008;14(5):1310–6.
[123] Martinelli A, D'Ilario L, Francolini I, Piozzi A. Water state effect on drug release from an antibiotic loaded polyurethane matrix containing albumin nanoparticles. Int J Pharm January 2011;407:197–206.
[124] Das B, Chattopadhyay P, Upadhyay A, Gupta K, Mandalc M, Karak N. Biophysico-chemical interfacial attributes of Fe_3O_4 decorated MWCNT nanohybrid/bio-based hyperbranched polyurethane nanocomposite: an antibacterial wound healing material with controlled drug release potential. New J Chem May 2014;38:4300–11.
[125] Pinto FCH, Cunha AS, Pianetti GA, Ayres E, Orefice RL, Silva GRD. Montmorillonite clay-based polyurethane nanocomposite as local triamcinolone acetonide delivery system. J Nano Mat 2011;2011. 11 pp.
[126] Langer R, Vacanti JP. Tissue engineering. Science May 1993;260(5110):920–6.
[127] Wang X, Lin P, Yao Q, Chen C. Development of small-diameter vascular grafts. World J Surg March 2007;31:682–9.
[128] Sharifpoor S, Labow RS, Santerre JP. Synthesis and characterization of degradable polar hydrophobic ionic polyurethane scaffolds for vascular tissue engineering applications. Biomacromolecules October 2009;10:2729–39.
[129] Wang MC, Lin JJ, Tseng HJ, Hsu SH. Characterization antimicrobial activities and biocompatibility of organically modified clays and their nanocomposites with polyurethane. ACS Appl Mater Interfaces November 2012;4:338–50.
[130] Shen H, Zhang L, Liu M, Zhang Z. Biomedical applications of graphene. Theranostics March 2012;2(3):283–94.
[131] Chetta GE, Lloyd JR. The design, fabrication and evaluation of a tri-leaflet prosthetic heart valve. J Biomech Eng June 1980;102:34–41.
[132] Imamura E, Kaye MP. Function of expended–polytetrafluoroethylene laminated tri-leaflet heart valve in animals. Mayo Clin Proc December 1977;52:770–5.
[133] Nistal F, García MV, Arbe E, Fernández D, Artiñano E, Mazorra F, et al. In vivo experimental assessment of polytetraflouroethylene tri-leaflet heart valve prosthesis. J Thorac Cardiovasc Surg June 1990;99:1047–81.
[134] Dias RCM, Goes AM, Serakides R, Ayres E, Orefice RL. Porous biodegradable polyurethane nanocomposites : preparation, characterization and biocompatibility tests. Mat Res June 2010;13(2):211–8.
[135] Kannan RY, Salacinski HJ, De Groot J, Clatworthy I, Seifalian AM, et al. The antithrombogenic potential of a polyhedral oligomeric silsesquioxane (POSS) nanocomposite. Biomacromolecules January 2006;7(1):215–23.
[136] Kannan RY, Salacinski HJ, Odlyha M, Butler PE, Seifalian AM. The degradative resistance of polyhedral oligomeric silsesquioxane nanocore integrated polyurethanes: an in vitro study. Biomaterials March 2006;27(9):1971–9.
[137] Kannan RY, Salacinski HJ, Ghanavi JE, Narula A, Seifalian AM, et al. Silsesquioxane nanocomposites as tissue implants. Plast Reconstr Surg May 2007;119(6):1653–62.
[138] Sarkar S, Burriesci G, Wojcik A, Aresti N, Hamilton G, Seifalian AM. Manufacture of small calibre quadruple lamina vascular bypass grafts using a novel automated extrusion-phase-inversion method and nanocomposite polymer. J Biomech April 2009;42(6):722–30.
[139] Khan F, Dahman Y. A novel approach for the utilization of biocellulose nanofibres in polyurethane nanocomposites for potential applications in bone tissue implants. Des Monomers Polym April 2012;15(1):1–29.